Heliyon 10 (2024) e33280

Contents lists available at ScienceDirect

Heliyon

journal homepage: www.cell.com/heliyon

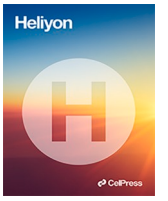

Research article

New proportion of levofloxacin citrate: Structural, physicochemical properties, and potency studies

Ilma Nugrahani [a,*], Hidehiro Uekusa [b], Hironaga Oyama [b], Agnesya Namira Laksana [a]

[a] School of Pharmacy, Bandung Institute of Technology, West Java, 40132, Indonesia
[b] Departement of Chemistry, School of Science, Tokyo Institute of Technology, Tokyo, 152-8551, Japan

ARTICLE INFO

Keywords:
Levofloxacin
Citric acid
Salt
Levofloxacin citrate 2-1
Hydrate
Stability
Solubility
Potency

ABSTRACT

Stability and potency improvement have been reported by reacting levofloxacin (LF) with citric acid (CA) in a (1:1) molar ratio. However, CA is known to be irritant to the gastrointestinal tract and should be minimized. In a novel approach, this experiment aimed to prepare LF – CA salt with reduced CA, the (2:1) molar ratio, study the structure, and investigate its solubility, stability, and potency improvement. Solvent-dropped grinding and slow evaporation methods were used to prepare the new ratio composition salt, characterized by electrothermal, differential scanning calorimetry, and powder X-ray diffractometry to confirm the physically new solid-state formation. Next, Fourier transform spectrophotometry identified the chemical interaction between LF and CA. After that, a comprehensive structural study using single-crystal X-ray diffractometry determined the 3D structure of the new salt, which determined the solid physicochemical behavior. Finally, stability, solubility, and potency tests were done to investigate the benefits of the new LF-CA composition. As a result, this experiment successfully synthesized the salt, which bound 4.5 water molecules, named LFCA (2:1) - 4.5 hydrate. This new solid-state salt was comparable with the established (1:1) molar ratio in solubility, stability, and potency, higher than LF alone. Hereafter, with a reduced CA portion, this new composition holds potential for further development in drug formulation as a stable, safer, and more efficient antibiotic.

1. Introduction

Broad-spectrum fluoroquinolone antibiotics have become one of the primary choices for treating infections caused by various bacteria. One is levofloxacin (LF), the second generation of fluoroquinolone, delivered in a single daily dose [1], indicating its high effectiveness. Structurally, LF has an OH group, making it more soluble than the previous generation in one group, i.e., ciprofloxacin. Still, on the other hand, that antibiotic is unstable towards humidity and lighting [2,3] due to the more opened N-methyl piperazine ring, causing it to be more reactive to the oxidative reaction and hydrolysis. Some reports reveal that masking this site may improve its stability, such as LF-DHBA [4].

In the solid form, LF exhibits two kinds of hydrate form, hemihydrate (LFH) and monohydrate (LFM) [5], and three anhydrous polymorphs, α, β, and γ [6]. Those forms cause a variety of LF's physicochemical properties, especially solubility and hygroscopicity

* Corresponding author. Ilma Nugrahani School of Pharmacy, Bandung Institute of Technology Jl. Ganesha 10, Tamansari, Bandung, West Java, 40132, Indonesia.
E-mail address: ilma_nugrahani@itb.ac.id (I. Nugrahani).

https://doi.org/10.1016/j.heliyon.2024.e33280
Received 19 October 2023; Received in revised form 18 June 2024; Accepted 18 June 2024
Available online 19 June 2024

[7], and may also influence the drug's dose by the hydrate transformation. Solid-state development may arrange the preferred structure for better physicochemical properties, including combining the drug with another substance by non-covalent reactions. The multi-component arrangement uses low-energy interactions, such as hydrogen or ionic bindings, which have not altered the pharmacological effect and have been used for decades [8,9]. Drugs may be tailor-made to fulfill a specific purpose by salt [10] and cocrystal [11] formation. Fluoroquinolone antibiotics have also been widely combined with other molecules by that strategy. For example, ciprofloxacin combined with non-steroidal anti-inflammatory drugs (NSAIDs) to improve both side's physicochemical properties, i.e., solubility [12]. Interestingly, some antibiotic multi-components show better antimicrobial activity than their parent drug, such as ciprofloxacin – picolinic acid [13] and ciprofloxacin – thiobarbituric and barbituric acid [14]. Next, some authors reported LF - metacetamol [15] and stearic acid [16], which improved LF's photostability and hygroscopicity and masked its unpleasant taste.

Recently, LF has been reported to react with antioxidant citric acid (CA), producing LFCA (1:1), which showed better stability and solubility than single LF. In addition, the salt increased the antibiotic potency, which was related to the permeability character change [17]. Structurally, LF is an amphoteric compound with an amine piperazine site as the proton acceptor (pKa = 8.07) and carboxylic moiety as the donor or acidic site (pKa = 5.33). Hereafter, it can be expected to react with any basic or acid counterion. CA is a stable antioxidant [18] with many potential binding sites from the three carboxylic moieties (pKa1 = 3.13, pKa2 = 4.76, and pKa3 = 6.40), making it reactive towards LF [19]. Besides, CA is freely soluble in water under ambient conditions [20] and economical, adding the advantages of this substance to be combined with LF. However, CA causes side effects on the gastrointestinal tract, such as irritation and acidosis [21].

This research aimed to develop a new LF-CA salt composition with less CA portion than (1:1), characterize and determine its three-dimensional structure, and investigate the stability and potency improvement. The combination salt was prepared using solvent-dropped grinding (SDG) and slow evaporation (SE) techniques. After that, the new solid-state product was characterized by thermal analysis (electrothermal and differential scanning calorimetry/DSC) and powder X-ray diffractometry (PXRD). Next, Fourier transform infrared (FTIR) was utilized to determine the new salt structure, completed with three-dimensional structure analysis by single-crystal X-ray diffractometry (SCXRD) [22].

Comprehensive solid structure determination was needed to explain the improvement in physicochemical properties, which would be empirically confirmed by stability, solubility, and antibiotic potency tests. All data supported the development of the new composition salt, LFCA (2:1). It was then studied comprehensively on its physicochemical properties and potency improvement as valuable information for further salt of drug combination by solid phase engineering. In addition, the three-dimensional structural data of this salt was hoped to enrich the structural scientific catalog.

2. Materials and methods

2.1. Materials

This experiment used levofloxacin (LF) hemihydrate (99.0 %), citric acid (CA) in monohydrate form (98 %), methanol (99 %), the reagent for phosphate buffer solutions: sodium chloride/NaCl (99 %), chloride acid/HCl (99 %), dihydrogen potassium phosphate (99 %), disodium hydrogen phosphate (99 %), sodium hydroxide (99 %), sodium acetate (99.7 %), and acetic acid glacial (99.7 %), potassium bromide/KBr crystal (>99 %) for infrared analysis, nutrient agar, plate count agar, and physiological sodium chloride solution were purchased from Sigma - Merck (Jakarta, Indonesia); all were purchased from Sigma (Bandung, Indonesia) in the pro analysis quality (99.0–99.9 %). This experiment also used aluminum plates and lids from Rigaku (Tokyo, Japan) for DSC thermal analysis and capillary tubes from Prima Medica (Bandung, Indonesia) for electrothermal analysis. Next, the brain heart infusion broth, Mueller Hinton broth, and Mueller Hinton agar were bought from Oxoid (Jakarta, Indonesia); and 0.5 McFarland standard solution from BioMerieux (Jakarta, Indonesia). Meanwhile, the distilled water, *Staphylococcus aureus* ATCC 25953, and *Escherichia coli* ATCC 9001 were prepared by the Bandung Institute of Technology Laboratory (Bandung Indonesia).

2.2. Methods

The experiment included salt preparation, solid-state characterization, and structure determination using FTIR and SCXRD, which were continued by solubility, stability, and potency tests. As explained in the Introduction, structurally, CA has three carboxylic acids [19], so it was possible to react with 3 or 2 M of LF equally beside the established one, LF – CA, in a (1:1) molar ratio. Hereafter, the (3:1) and (2:1) molar ratios of LF – CA salts were screened, but only the LF – CA (2:1) showed a positive result in the experiment condition; then, only this composition was experimented further.

2.2.1. The physical mixture (PM) and salt preparation

The PM of LFCA was prepared by gently mixing LF (2 mEq) and CA (1 mEq) with a mortar and stamper, and this was used as a reference besides the single compounds. Next, LFCA (2:1) salt was prepared by solvent-dropped grinding (SDG) and slow evaporation (SE) methods. Firstly, LF and CA were mixed in a 2:1 M ratio. The mixture was then ground using mortar and stamper with 70 % aqueous methanol until wet and homogenous, repeated 2–3 times, and let dry under ambient conditions. After that, half of the SDG product was stored, and the remaining solid sample was dissolved with aqueous methanol 70 % until clear (~20 mL for 250 mg mixture), filtered, collected in a 50 mL volume of Erlenmeyer tube from Pyrex (Illinois, USA), and then the solvent was slowly evaporated under the ambient condition (25 ± 5 °C/70–80 % RH) to collect the clear crystals. The preparation was replicated in more

than six batches. The physical mixture and salts from SDG and SE were characterized by solid analysis instruments, including electrothermal, DSC, PXRD, and FTIR. The salts showed similar data, but SDG is more affordable in producing more salt more simply and efficiently. Therefore, the SDG product was used for solubility, stability, and potency tests; meanwhile, the nice crystal from slow solvent evaporation was used to determine the three-dimensional structure using SCXRD.

2.2.2. Physical characterization using solid analysis instruments

2.2.2.1. Electrothermal measurement. The powder/crystal of starting materials, PM, and LFCA samples were measured using Electrothermal AZ 9003 (Staffordshire, UK) until their melting/degradation point. A small amount of the mixture was filled into a capillary tube with one side closed. The heating rate was set at 10 °C/min, and the melting point and physical changes were recorded by observing via the observer hole.

2.2.2.2. DSC analysis. DSC analysis was conducted using a Rigaku Thermoplus EVO2-DSC8231 (Tokyo, Japan) to confirm the new solid–state formation, which a unique thermogram should present, differs from the starting materials. The endothermic peaks belonged to hydrate release and melting point; meanwhile, the exothermic curve showed recrystallization or degradation. In this experiment, ~2 mg of the sample was filled into a DSC alumina pan covered with a lid and pressed to close it tightly. Then, it was put in the sample holder beside an empty alumina pan as a reference. Like in the electrothermal method, DSC measurement started from the ambient temperature with a heating rate of 10 °C/min until each predicted melting/degradation point.

2.2.2.3. PXRD analysis. PXRD was used to identify the new solid-state structure from LFCA (2:1). The sample in powder form was spread in a glass sample holder between the Mylar films. Next, the diffraction was measured at 2θ with intervals of 3–40° and a scan speed of 0.01–3°/min, using Cu-Kα radiation with a graphite monochromator using PXRD Rigaku Miniflex (Tokyo, Japan). The instrument was operated using a voltage of 40 kV and a current of 35 mA.

2.2.2.4. Microscope observation. Each starting material and SDG product was recrystallized using aqueous methanol (90 %) under ambient conditions (25 ± 5 °C/70–80%RH). The dry crystals were then observed visually using a binocular microscope Olympus CX21 (Tokyo, Japan) at 40x magnification, and the picture was taken using an iPhone 12 camera (Canada, USA).

2.2.3. Structural study

2.2.3.1. FTIR analysis. The solid sample was mixed with KBr in a ratio of 1:100 and ground gently in a marble mortar until homogeneous. Next, it was compressed using a hydraulic press to make a transparent and clear disc plate. After that, the plate was inserted into the sample holder of an FTIR Jasco 4200 Type-A (Oklahoma City, USA). The spectra were scanned at 4000–400 cm^{-1} under the 4 cm^{-1} resolution. The salt formation will be shown by the spectra change at 1500-1700 cm^{-1} [22].

2.2.3.2. SCXRD analysis. The suitable LFCA (2:1) single crystal from the SE technique, which was clear and had an appropriate diameter (~0.5–1.0 mm), was selected using a microscope binocular and put in the SCXRD XtaLAB Synergy-DW sample holder, Rigaku (Tokyo, Japan). The crystal measurement was conducted in ω-scan mode, using a Cu Kα radiation (λ = 1.54184 Å) rotating anode source with a focusing mirror under −180 °C.

2.2.4. Software

Microsoft Excel 365 composed the phase diagram from the electrothermal, thermogram from DSC, diffractogram from PXRD, and infrared spectra from FTIR. Next, the SCXRD measurement result was integrated and scaled using CrysAlis^{Pro} software. Afterward, the SHELXT and SHELXL software was used to solve and refine the crystal structure, which was then drawn by the Mercury 4.3.1 program. The nonhydrogen atoms were refined anisotropically, and the hydrogen atoms were found on a different Fourier map. All hydrogens of CH were placed using geometric calculations and treated by a riding model. The OH hydrogen positions were refined with fixed thermal parameters except for water molecule O-39, which has two H atoms on calculated positions using the hydrogen bonding scheme. NH^{+}'s hydrogens were refined freely to confirm the cation state of LF. The anion state of CA was established by C–O lengths. There are minor disorders in the carboxylic group of CA.

2.2.5. Stability test

The physical stability study was conducted under controlled conditions. 500 mg of LF and LFCA (2:1) were observed on a Petri dish exposed to direct sunlight in the opened air in Bandung, Indonesia (25 ± 5 °C/70–80 % RH). The color change was observed, and LF content was determined using spectrophotometry UV–visible weekly for four weeks. The iPhone camera recorded the color change every week. PXRD and FTIR were also used to monitor the physical and chemical modifications during the stability test [15]. The chemical stability of LF was investigated by quantifying the content using a verified method of spectrophotometer UV Beckman DU640 UV/Vis Spectrophotometer (Indianapolis, Indiana, USA) under λ = 331 nm using water pH 7.0 as the solvent [17]. The stability test observed three batches of LFCA (2:1) product, and the UV absorption measurement was replicated three times for each sample solution.

2.2.6. Solubility test

The solubility value of LFCA (2:1) in water and phosphate buffer solution pH 6.8 and 7.4 were determined and compared to LF's, representing the gastrointestinal track condition. Buffer solution pH 6.8 was made from 6.8 g dihydrogen potassium phosphate (KH_2PO_4) mixed with 1g sodium hydroxide (NaOH) and dissolved in 1L of distilled water. A few drops of NaOH solution 0.05 N were added to adjust until the final pH was measured using a pH meter Mettler Toledo (Darmstadt, Germany) [23]. Next, buffer phosphate solution pH 7.4 was made from 1.179 g of dihydrogen potassium phosphate (KH_2PO_4) was dissolved with 4.303g of disodium hydrogen phosphate (Na_2HPO_4) and 9g of sodium chloride in 500 mL of distilled water. Then, the solution was adjusted to the pH (7.4) by dropping a few NaOH 0.05 N and checked by a Mettler Toledo's pH meter (Darmstadt, Germany) [23].

The samples were filled into 10 mL Erlenmeyer tubes, added by each medium (water, buffer phosphate pH 6.8 and 7.4 represented gastric and ileum environment respectively), closed, and shaken at 25 rpm at room temperature. The solid sample was added until some powders remained undissolved, indicating a saturated condition. Afterward, the LF solubility was determined using verified UV spectrophotometry under $\lambda = 331$ nm by a Beckman DU640 UV/Vis Spectrophotometer (Indiana, USA), the same as the stability test method [17].

2.2.7. Antimicrobial test

The improvement in antimicrobial capability was evaluated by minimum inhibitory concentration (MIC) and equivalence-potency tests [4,24,25], comparing the LFCA (2:1) system to the single components. Firstly, all samples were dissolved in pH 7.0 (water) and phosphate buffer solutions, pH 6.8 and pH 7.4, similarly to the solubility test solutions.

2.2.7.1. MIC determination. MIC measurement was conducted to determine the minimum concentration of antibiotic needed to inhibit the growth of bacteria. This parameter represented the strength of the antimicrobe. Before the main experiment was performed, the medium's capability to grow bacteria was checked by a fertility test. First, a microdilution tray was arranged by twelve columns and eight rows of tiny tubes. Next, each tube was filled with 100 μL of the mixed solution of medium and buffer solution pH 6.8 and 7.4 in the ratio (1:1). Then, 10 μL of bacterial inoculum was added into each tube. After that, one tube of 100 μL of culture medium buffer (1:1) with 10 μL of bacterial inoculum (positive control) and one tube of 100 μL of culture medium buffer (1:1) without bacterial inoculum was the negative control. The microdilution tray was then incubated for three days at 37 °C, and the bacterial growth was observed by checking the turbidity of the mixture in the tubes visually using a magnifying glass (Insten Magnifying Glass 10 × Handled, Hereford, UK) [24].

Next, the liquid microdilution method using Mueller Hinton broth (CLSI 2006) was conducted to measure the MIC value of LFCA (2:1) and both starting components, using a tray with twofold sample-dilution steps. The tube capacity was ~300 μL, and according to CLSI guidelines, the medium and bacterial inoculum were used in small amounts, which were ~100 μL and 10 μL, respectively [24]. The 100 μL sample was dissolved in buffer pH 6.8 and 7.4 and filled into the tubes in 100 μL. Next, the twofold serial dilution was prepared at 20–0.039 μg/mL of sample. After that, 100 μL of medium and 10 μL of bacterial inoculum with a concentration equivalent to the 0.5 McFarland standard (1.5×10^8 colonies/mL) were added into the tubes. For the positive control, one tube of 100 μL medium-buffer solution (1:1) and 10 μL bacterial inoculum. Meanwhile, one tube of 100 μL medium and buffer (1:1) without bacterial inoculum was used as the negative control. All tubes were then incubated at 37 °C for 24 h, and the bacterial growth was observed to compare with the negative and positive control. The MIC was determined by observing the lowest concentration, which did not show bacterial growth. The antimicrobial potency test was conducted on *Staphylococcus aureus* (Gram-positive) and *Escherichia coli* (Gram-negative) [24].

2.2.7.2. Equivalence-potency test. This testing aimed to compare the potency of the salt form/LFCA (2:1) to the parent antibiotic/LF. First, Mueller Hinton medium was poured into a Petri dish and inoculated with 100 μL of a 0.5 McFarland bacterial turbidity. Next, the 6.0 mm metal cylinders were placed on the agar plate. Afterward, the metal cylinders were filled with 100 μL of each sample solution

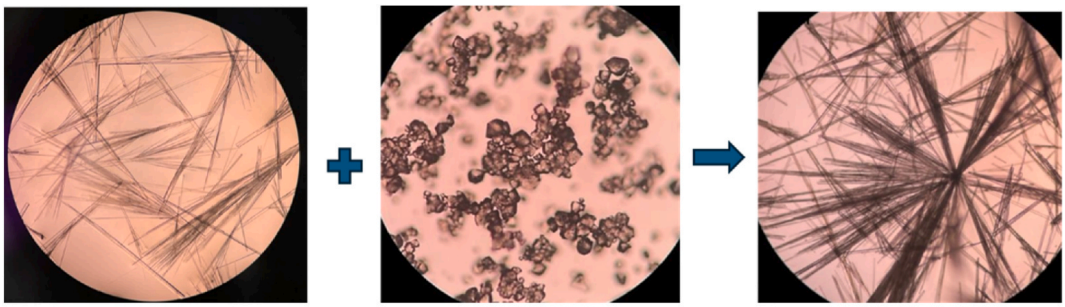

Fig. 1. The habit of LF, CA, and LFCA (2:1) multicomponent system from solvent evaporation method using 70 % methanol.

equal to LF concentrations of 10.24, 12.8, 16, 20, and 25 μg/mL (S1–S5) in six replicates. All Petri dishes were then stabilized and incubated at 37 °C for 24 h. After the incubation period, the inhibition zone diameters were measured. Finally, the potency of LFCA and PM was calculated by plotting the log of concentration versus inhibition diameter, and the inhibition strength of the middle concentration (S3), 16 μg/mL, was determined and compared to LF [25].

3. Results

3.1. LFCA (2:1) salt preparation and characterization

This experiment was purposed to make the LFCA salt with a lower portion of CA than (1:1). Based on its structure, CA has three carboxylic acid moieties to react with three counterions. Hence, the LF – CA (3:1) and (2:1) were screened promptly. However, only the (2:1) molar ratio showed a positive result in this experimental condition. Thus, only that molar ratio was experimented with further.

From the previous screening, SDG produced the white powder; meanwhile, SE yielded white needle-like crystals, as shown in Fig. 1. The electrothermal characterization on both products showed that LFCA (2:1) turned from light-yellow to dark chocolate, indicating it oxidized before melting at 225 °C. This data was then confirmed by the DSC thermograms in Fig. 2, which also showed an endothermic peak at 225 °C. In addition, the thermogram showed an endothermic peak at 83 °C, predicted as the water release peak. Those data are significantly different from the starting material thermal profile. LF (hemihydrate) melted at 229 °C and then decomposed, as shown in its thermogram in Fig. 2. Meanwhile, CA showed that the water molecules released at 76 °C confirmed the hydrate form and then melted with decomposition after 145 °C. Hence, the thermal data proved the production of a new solid-state phase with a distinctive habit [22,26,28].

Afterward, the solid-state characterization confirmed and described the new solid-state multicomponent phase. PXRD analysis investigated the new solid phase arrangement by comparing the LFCA (2:1) diffractogram with the starting component's profile in Fig. 3. LFCA (2:1) diffractogram showed the new significant peaks at $2\theta = 9.32$, 10.18, 11.24, 12.34, and 20.98°; total difference without any origin peaks from the starting materials (LF and CA) remained, strengthening the DSC data of a new solid phase [22,26,28]. Six batches of SGD and SE products have similar thermograms and diffractograms, meaning both methods produced the same solid phase structure.

3.2. Structural study

The experiment continued with the two-dimensional structure study using FTIR to confirm the ionic interaction site between LF and CA, followed by SCXRD to solve the 3D structure of LFCA (2:1). The complete structural data might support the explanation of the improvement in physicochemical properties.

3.2.1. Two-dimensional structural study

Fig. 4 shows overlapped infrared spectra of LF and CA in the PM (2:1) data, with –OH broad bands. Meanwhile, LFCA (2:1) presents a band at 3421 cm^{-1}, which came from the 3251 cm^{-1} shifting of LF. Also, the LF's peak at 2931 cm^{-1} disappeared, but 3039 cm^{-1} existed in the LFCA salt's spectra, reflecting the shifting bands of the N–H band of LF, which bound with the hydroxy bond of CA [4,17,

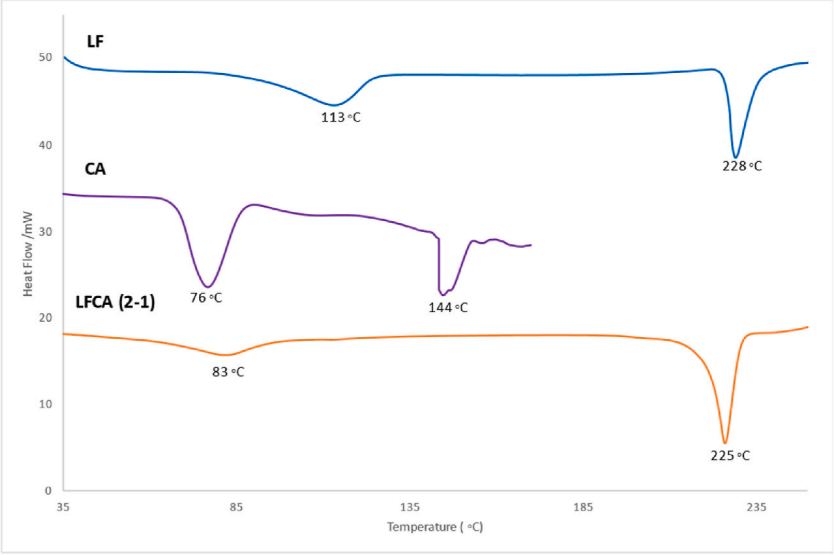

Fig. 2. DSC Thermogram of LFCA (2:1) and the starting materials. *(n = 3)*.

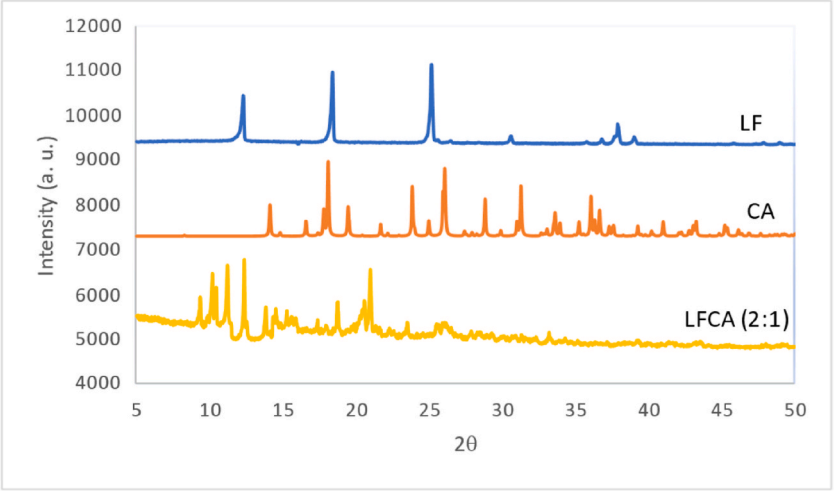

Fig. 3. PXRD diffractogram of LFCA (2:1) and its starting materials, LF (hemihydrate) and CA (citric acid). *(n = 3)*.

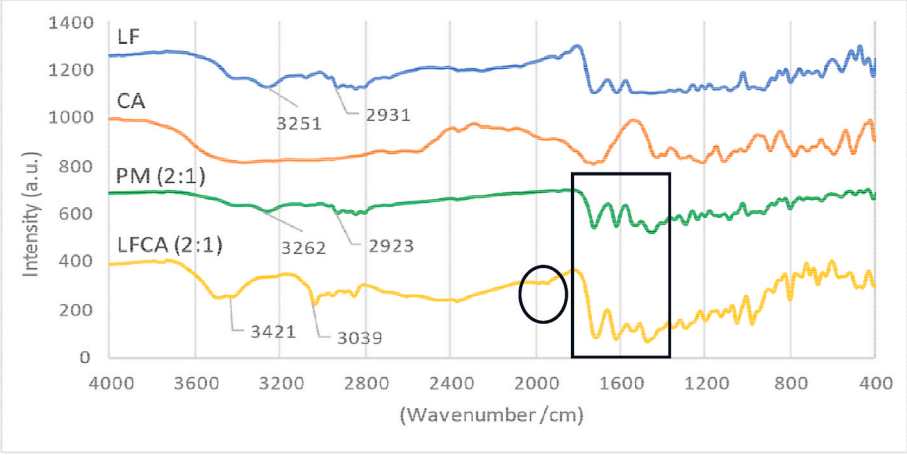

Fig. 4. FTIR spectra of LFCA (2:1), PM (2:1), and its starting materials: CA (citric acid) and LF (levofloxacin hemihydrate). *(n = 3)*.

Table 1
Crystal data of LFCA (2:1) 4.5 hydrate.

Structure Name	Levofloxacin Citrate (2:1) 4.5 hydrate
Empirical formula	$C_{42}\ H_{57}\ F_2\ N_6\ O_{19.5}$
Formula weight	995.93
Crystal system	Monoclinic
Space group	$P2_1$
a/Å	9.5778 (3)
b/Å	37.2950 (12)
c/Å	13.3709 (5)
α/°	90
β/°	106.734 (3)
γ/°	90
V/Å^3	4573.9(3)
Z	4
Density (calculated)/g cm^{-3}	1.466
R/%	3.77
CCDC Deposition Number	2221876

22,28]. Next, a new peak at ~1900 cm^{-1} describes the environmental change of the methyl amine of LF, which interacted with the C═O of CA (in Fig. 4 is signed by a circle) and between 1500 and 1750 cm^{-1} (signed by rectangular signed area).

Furthermore, LFCA (2:1) spectra had a broader band at 3500-2800 cm^{-1}, indicating the hydrate form [5–7], which was in line with DSC data in Fig. 2. The data was consistent among the three replicate measurements. Based on the significant changes in spectra, the formation of a salt structure could be predicted rather than a cocrystal, with some water molecules bonded [22,28]. SCXRD will then comprehensively elaborate on this data.

3.2.2. *Three-dimensional (3D) structural study*

An acceptable and appropriate size of a single crystal of the SE product was analyzed and successfully determined by SCXRD analysis to be 4.5 hydrate form (LF-CA-water = 4:2:9), producing comprehensive data in Table 1 and Supplementary 1. The structural drawing in Fig. 5 reflects that all CAs became di-anionic, and the N terminal of piperazine of LF took additional protons to be cationic. Part of the carboxylic group of CA and one crystalline water molecule showed disorder. Fig. 5a depicts the crystal structure of LFCA (2:1) with hydrogen bonds indicated by the blue mark. Three of four NH of LF form hydrogen bonds with the carboxylate of CA, and the remaining are with the water molecules. Also, CA … CA, CA … water, water … water hydrogen bonds were observed.

Next, Fig. 5(b)–(d) show the crystal packing of LFCA (2:1) views along the a, b, and c axis. These views depict the hydrophobic layer, in which the hydrophobic portion of LF was stacked and alternated with the hydrophilic layers. Meanwhile, the charged sites of LF, CA, and water molecules were assembled by hydrogen bonding. This situation may support the stability and solubility of LF in this salt solid-state form.

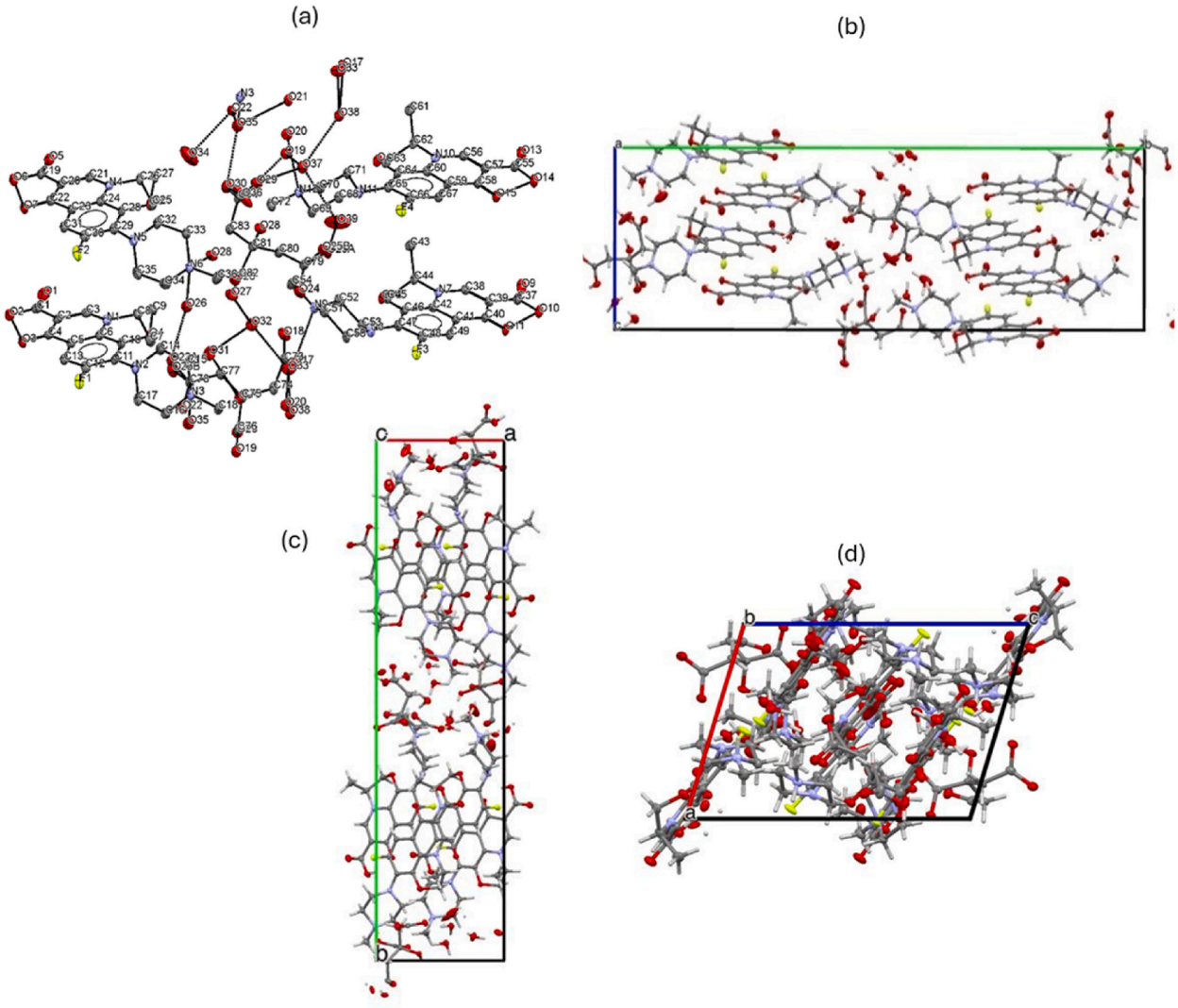

Fig. 5. Crystal structure of LFCA (2:1) 4.5 hydrate. (a), crystal packing of LFCA (2:1) from a-b view-sites (b), b-c view-sites (c), and a-c view-sites (d).

As a confirmation, the calculated and measured PXRD are shown in Fig. 6. The positions of the major peaks are consistent, indicating that the powder salt used in the measurements matches the LFCA (2:1) - 4.5 hydrate structural data.

3.3. Stability study

The physical stability observation results are shown in Fig. 7 (A-E) for LF and 8 (A-E) for LFCA (2:1), which presented the origin condition (Figs. 7A and 8A) and after the storage for 1,2,3,4 weeks (7 and 8 B, C, D, and E, respectively). Timely, the color of LF (hemihydrate) changes from light (Fig. 7A) to dark yellow (Fig. 7E); meanwhile, the salt did not transfer color as shown in no difference of Fig. 8 A, B, C, D, and E, respectively. Those pictures show that the stability of salt form was better than that of LF alone. Next, FTIR and PXRD traced the stability of LFCA (2:1) and LF powder toward humidity, like in the LF–metacetamol stability study [15].

Fig. 9A shows no bands or peak intensity changes at 2500-3900 cm^{-1}, and the steady of the broad of the bands is also the same, revealing no entrapped or releasing water in LFCA (2:1) over four weeks. Meanwhile, Fig. 9B depicts the bands and peak intensity changes of LF (hemihydrate) weekly, which shows that the peak intensity at 2500-3900 cm^{-1} became broader due to the addition of water molecules into the LF solid-state structure [5–7,28]. Based on the FTIR spectra, LFCA (2:1) – 4.5 hydrate was stable towards the humidity of the room conditions (25 ± 5 °C/70–80 % RH) for four weeks. It was probably caused by the thermodynamically robust water molecules in the inner layer of that solid multicomponent salt, which was confirmed by PXRD data in Fig. 10A and B.

On the other hand, during storage, LF hemihydrate changed to monohydrate from week 1 (Fig. 10A). Again, the salt's diffractogram was steady (Fig. 10B), which aligns with the FTIR data. Hence, it was proven that the salt's solid-state structure was stable under ambient conditions for that testing period, meaning it was more controllable than LF alone, considering that the hydrate transformation impacted the purity of the drug.

Furthermore, the content of LF in the salt sample was compared to LF alone for four weeks. It was checked by content determination using UV-spectrophotometry, and the result depicted in Fig. 11 shows that the LF hemihydrate content decreased by ~3.34 %. Regarding the FTIR and PXRD data, the hemihydrate state adsorbed water and transformed into hemihydrate since the first week, reflected by a ~2.5 % content decrease. Then, ~0.84 % of the remaining portion was related to the oxidative chemical degradation of LF under direct lighting. The data was processed from three times experiments and showed the same tendency. On the other hand, the LF level in the salt form did not change significantly.

Based on all stability data, LFCA (2:1) 4.5 hydrate was more stable than its parent drug, LF. The better stability of the salt form may relate to the ionic reaction neutralizing the responsible site of oxidation [3,4,15,17,27]. Besides, referring to the solid structure in Fig. 5, the outer position of CA in LFCA (2:1) covered the LF structure.

3.4. Solubility test

Generally, salt may improve the parent base or acid compound, as in the case of ciprofloxacin picolinate [13] and barbiturates [14]. In addition, the change of solid-state packing and position of the molecules in their three-dimensional conformation affects the solubility improvement. Hereafter, the solubility of LFCA was also tested. The LF's content measurement was done at λ-max = 331 nm, where CA had no absorbance.

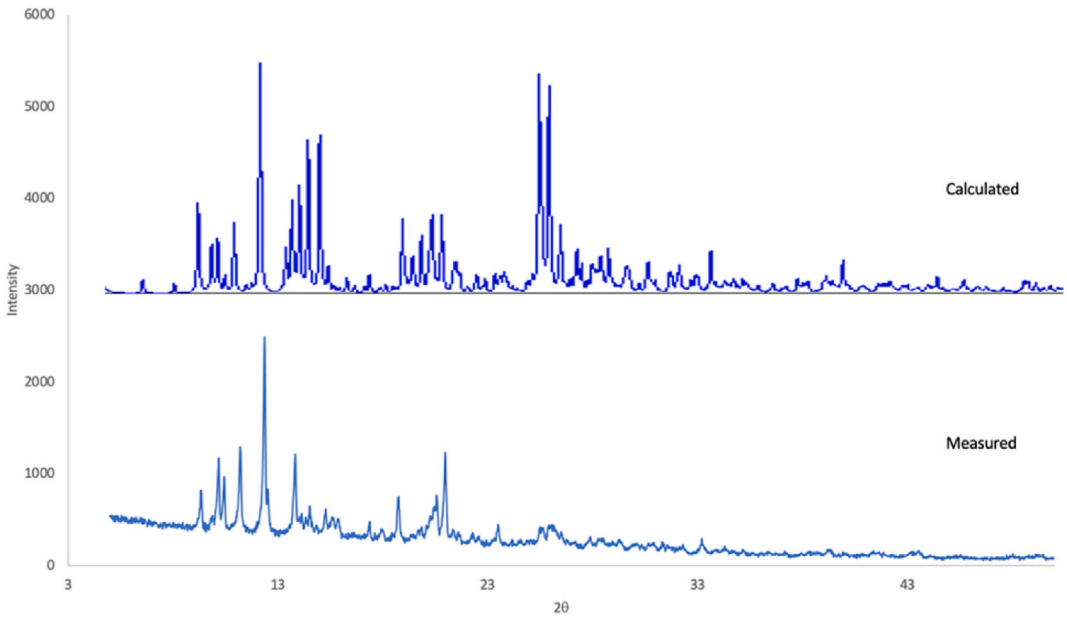

Fig. 6. Calculated and measured powder X-ray diffraction of levofloxacin citrate (2:1).

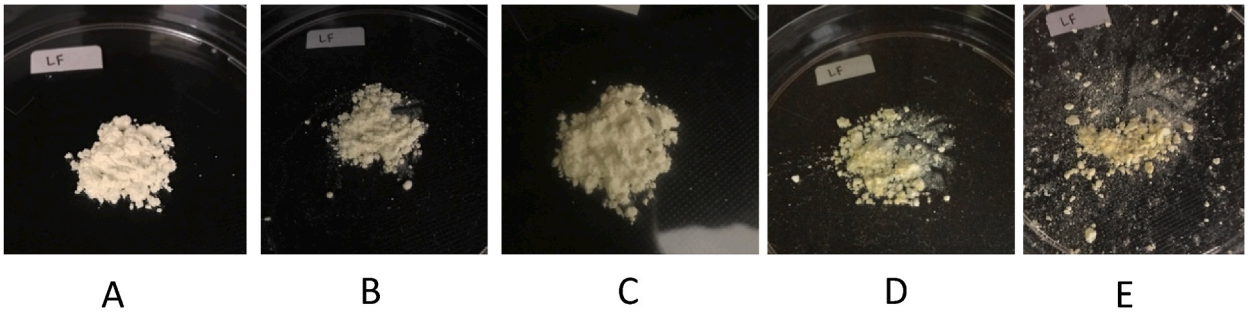

Fig. 7. Initial LF (A), and after the storage under (70–80%RH/25 ± 5 °C) for (B) one, (C) two, (D) three, and (E) four weeks.

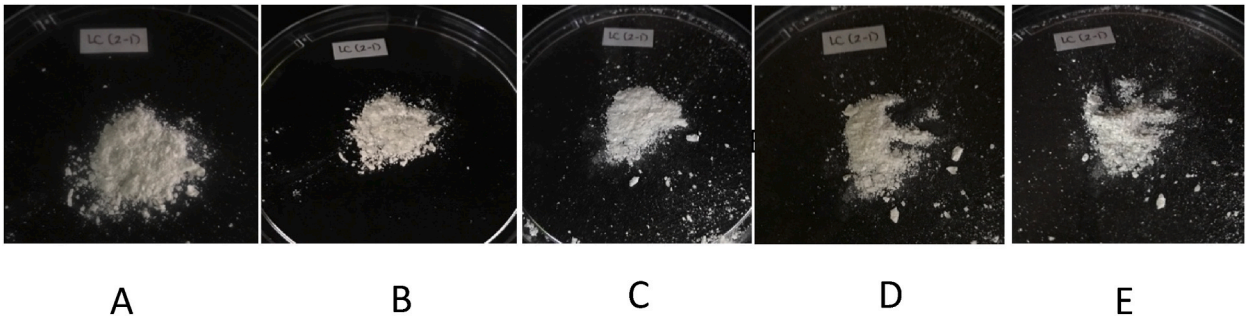

Fig. 8. Initial LFCA (2:1) (A), and after the storage under the direct lighting and opened air (70–80%RH/25 ± 5 °C) for (B) one, (C) two, (D) three, and (E) four weeks. *(n = 3)*.

Table 2 and the diagram in Fig. 12 show that the salt system has better solubility than LF alone in all pH media tested. In the water pH of 7.0 and buffer pH of 7.4 with a final pH of 6.35 and 6.75, respectively, the solubility increased ~2.1 times. However, in pH 6.8, with the final pH 5.73, the solubility improvement was 1.3 times only. Hence, pH may also be predicted to influence the salt phase's solubility. Many reports explained that the best environment for LF solubility is pH 6.5–6.7. Hereafter, the water and buffer solution with a final pH of 6.75 dissolved the salt more than the buffer with a pH under 6.0 [17]. Elaborating on the solid-state structure shown in Fig. 5, the hydrophobic layer of LF was stacked and alternated with the hydrophilic layers of CA. Moreover, CA, which forms a channel between the water and LF molecules, increases water absorption and solubility.

3.5. Antimicrobial study

Table 3 shows the lower MIC of LFCA (2:1) - 4.5 hydrate from three replicates, indicating that the salt was more effective in inhibiting *Staphylococcus aureus* (Gram-positive and *Escherichia coli* (Gram-negative), about ~2 times higher compared to LF alone. Next, Fig. 13shows the equivalency potency test results, comparing the salt with LF alone in a 16 μg/mL concentration. The new salt's potency toward Gram-positive bacteria *Staphylococcus aureus* (Fig. 13A) and Gram-negative *Escherichia coli* (Fig. 13B) was also ~1.5-2 times higher than that of LF, which equals the previous composition (LFCA 1:1) [17].

Those potency improvements may be caused by the polarity change, which made the drug more accessible to pass the antibiotic membrane. This potency increase phenomenon has also been reported from the salt reaction of ciprofloxacin with NSAIDs, such as mefenamic acid and ketoprofen, which showed a slight enhancement in antimicrobial activity toward *S. coli,* which was related to the solubility increase [12]. Also, the antibiotic potency improvement was reported to be shown by the ciprofloxacin salt with nicotinic and isonicotinic acid [29], as well as our previous research about LF – DHBA [4] and LF – CA (1:1) [17]. In addition, CA alone owned a minor antimicrobial potency and contributed synergistic effects in the salt form with LF [17,30–34].

Finally, based on all data, the LFCA (2:1) - 4.5 hydrate offers the same advantages of improving the solubility, stability, and antibiotic potency of LF as the established composition, LFCA 1:1. Moreover, this new composition was more efficient and safer due to the smaller CA dose, which may reduce its side effects [35].

4. Conclusion

This experiment successfully developed a new composition of levofloxacin citrate salt, namely LFCA (2:1) - 4.5 hydrate, which increased the solubility, stability, and potency of LF. This new solid salt structure bound the amine of methyl piperazine with the 1st and 2nd carboxylates of CA, covering the oxidative reactive site of LF to improve the stability. Meanwhile, 4.5 water molecules interacted with LF by hydrogen bonding, forming a canal hydrate in a monoclinic lattice system - $P2_1$. The hydrophobic layer of LF was

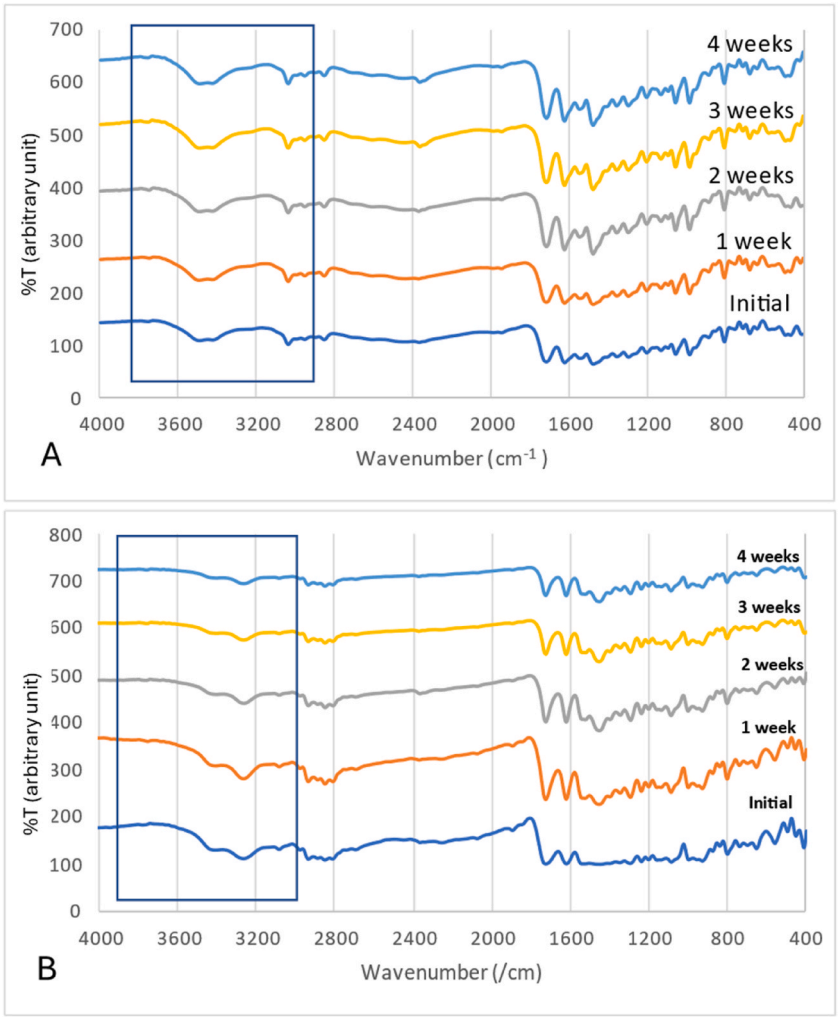

Fig. 9. FTIR spectra of levofloxacin (A) and levofloxacin citrate (2:1) (B) from the solid stability test under lighting ($n = 3$).

stacked and alternated with the hydrophilic layers of CA, causing the LF's solubility to increase (~1.3 times in the phosphate buffer pH 6.8–2.1 times in the water). Also, it improved LF's MIC and equivalency potency towards *Escherichia coli* and *Staphylococcus aureus* (~1.5–2 times), which means that it can be expected to handle the bacteria resistance. Hereafter, this LFCA (2:1) 4.5 hydrate is a potential antibiotic–antioxidant combination salt to be formulated further in various pharmaceutical dosage forms, such as tablet, syrup, and injection.

Funding statement

This research is funded by the Overseas Collaboration Research, World Class University Program, Research and Community Service Institution, Bandung Institute of Technology, Indonesia, number: 4949/IT1.B07.1/TA.00/2022 (I.N.); and JSPS KAKENHI, Japan, Grant number JP20H04661 and JP22K05032 (H.U.).

Data availability

The article presents all the main data. The cif data of crystal structure and Supplementary 1, which was deposited in CCDC (Cambridge Crystallography Data Center) number 2221876.

CRediT authorship contribution statement

Ilma Nugrahani: Writing – review & editing, Writing – original draft, Visualization, Validation, Supervision, Software, Resources, Project administration, Methodology, Investigation, Funding acquisition, Data curation, Conceptualization. **Hidehiro Uekusa:**

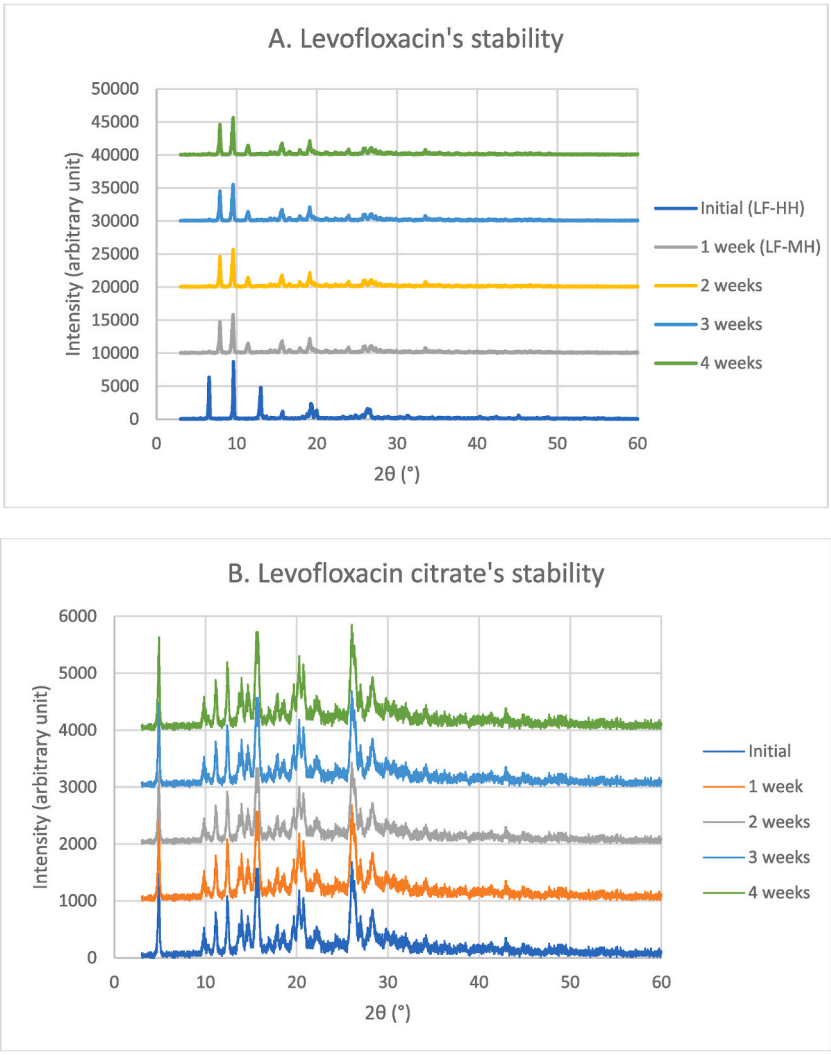

Fig. 10. Diffractogram of LF (A) and LFCA (2:1) (B) from stability test ($n = 3$).

Writing – review & editing, Writing – original draft, Visualization, Supervision, Software, Resources, Methodology, Funding acquisition, Data curation. **Hironaga Oyama:** Writing – original draft, Visualization, Software, Investigation, Formal analysis, Data curation. **Agnesya Namira Laksana:** Writing – original draft, Visualization, Methodology, Investigation, Formal analysis, Data curation.

Declaration of competing interest

The authors declare that they have no known competing financial interests or personal relationships that could have appeared to influence the work reported in this paper.

Abbreviation

CA	Citric acid
DSC	Differential Scanning Calorimetry
FTIR	Fourier Transform Infrared
h	hour
HCl	Hydrogen chloride
KH_2PO_4	dihydrogen potassium phosphate
KBr	Sodium bromide
LF	Levofloxacin

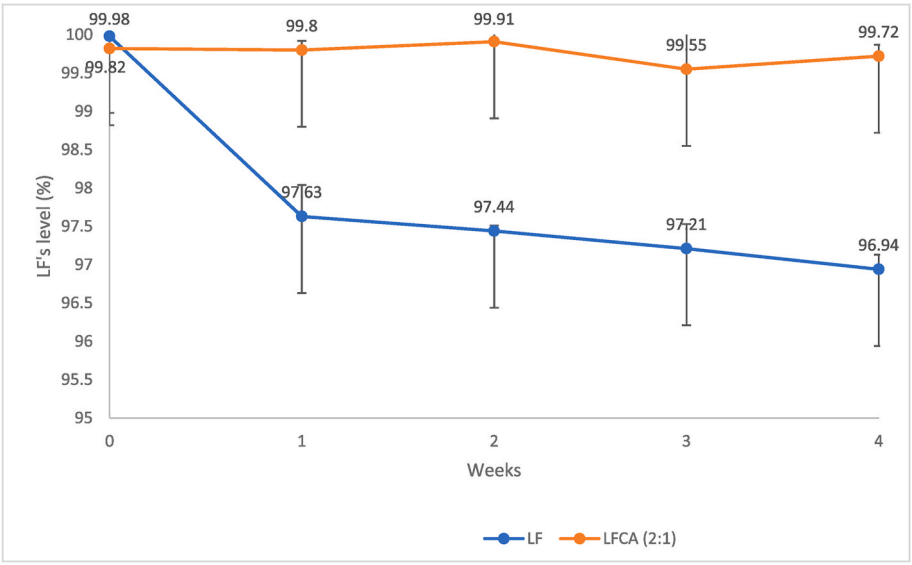

Fig. 11. Levofloxacin's content from the stability test of the single component and levofloxacin citrate/LFCA (2:1) 4.5 hydrate ($n = 3$).

Table 2
Solubility of LF and LFCA 2-1 in medium water pH 7.0, pH 6.8, and 7.4. *($n = 3$).*

Sample	Solubility (mg/mL)		
	in water pH 7.0	in pH 6.8	in PH 7.4
LF (base)	88.4 (final pH 6.82)	99.2 (final pH 6.74)	66.3 (final pH 7.12)
LFCA (2:1) 4.5 hydrate	154.6 (final pH 6.35)	123.4 (final pH 5.73)	134.8 (final pH 6.75)

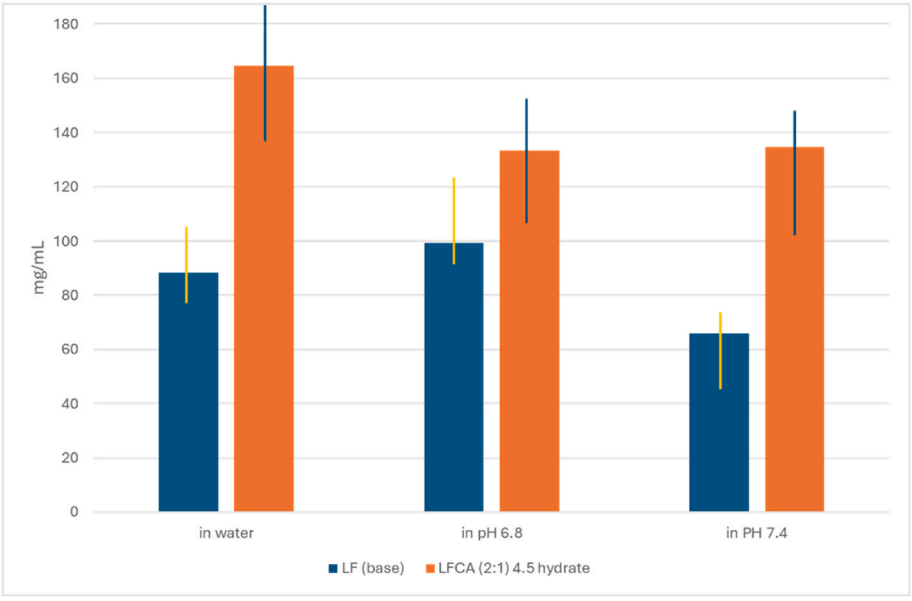

Fig. 12. Solubility test data of LF (levofloxacin base) and LFCA (levofloxacin citrate) (2:1) 4.5 hydrate. ($n = 3$).

LFCA Levofloxacin citrate
LFH Levofloxacin hemihydrate
LFM Levofloxacin monohydrate
meq Mole equivalent

Table 3
Microdilution – MIC data.

Sample	MIC toward Bacteria under Different pH (μg/mL)								
	S. aureus (9.7×10^8 Colony/mL)				*E. coli* (1.3×10^8 Colony/mL)				
	pH 6.8	pH 7.4			pH 6.8		pH 7.4		
	MIC	Final pH	MIC	Final pH	Final pH	MIC	Final pH	MIC	Final pH
LF	0.156	6.8	0.078	7.4	1.2	0.078	6.8	0.078	7.4
CA	>500	6.7	>500	7.2	1.2	>500	6.7	>500	7.3
LFCA 2:1	0.078	6.7	0.156	7.3	1.2	0.156	6.7	0.156	7.3

Note: LF: levofloxacin; CA: citric acid; LFCA: levofloxacin citrate; MIC: minimum inhibitory concentration. The experiment was done in triplicate (n = 3).

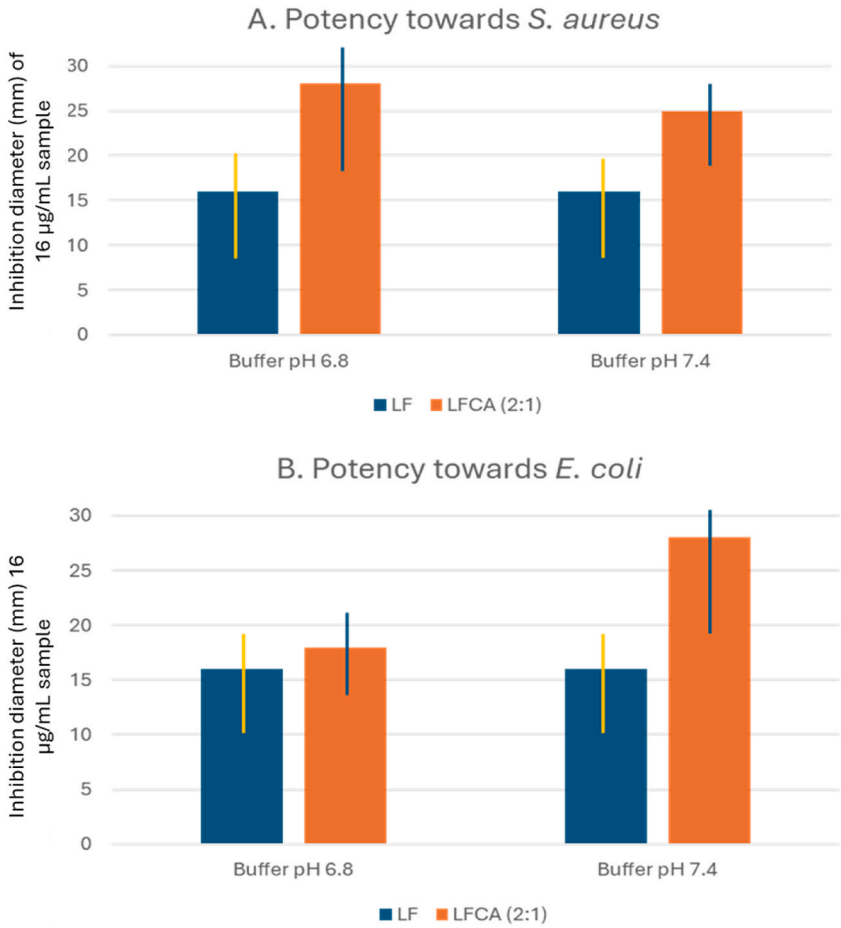

Fig. 13. Potency comparison between levofloxacin (LF) and levofloxacin citrate (LFCA) (2:1) 4.5 hydrate toward *Staphylococcus aureus* (A) and *Escherichia coli* (B) *(n = 6)*.

MIC	Minimum inhibitory concentration
mL	Milliliter
NaOH	Sodium hydroxide
Na_2HPO_4	Disodium hydrogen phosphate
OH	Hydroxyl
pH	Potential hydrogen
PXRD	Powder X-Ray Diffractometry
RH	Relative humidity
SCXRD	Single Crystal X-Ray Diffractometry

SDG	Solvent-dropped grinding
SE	Solvent evaporation
w/v	weight per volume
Å	Angstrom
°	Degree
°C	Degree Celsius
cm^{-1}	Inverse centimeter
λ	Lambda
L	Liter
μL	Microliter
%	Percent

Appendix A. Supplementary data

Supplementary data to this article can be found online at https://doi.org/10.1016/j.heliyon.2024.e33280.

References

[1] V. Podder, N.M. Sadiq, Levofloxacin. [Update 23 September 2022], in: *StatPearls*; StatPearls Publishing: Treasure Island, FL, USA, 2023. Available online: https://www.ncbi.nlm.nih.gov/books/NBK545180/. (Accessed 30 April 2023).
[2] S.V. Blokhina, A.V. Sharapova, M.V. Ol'khovich, T.V. Volkova, G.L. Perlovich, Solubility, lipophilicity and membrane permeability of some fluoroquinolone antimicrobials, Eur. J. Pharmaceut. Sci. 93 (2016) 29–37 ([CrossRef]).
[3] A. Czyrski, J. Sznura, The application of box-Behnken-design in the optimization of HPLFCA separation of fluoroquinolones, Sci. Rep. 9 (2019) 19458 ([CrossRef]).
[4] I. Nugrahani, M.R. Sulaiman, C. Eda, H. Uekusa, S. Ibrahim, Stability and antibiotic potency improvement of levofloxacin by producing new salts with 2,6- and 3,5-dihydrobenzoic acid and their comprehensive structural study, Molecules 15 (1) (2023) 124 ([CrossRef]).
[5] S.S. Singh, T.S. Thakur, New crystalline salt forms of levofloxacin: conformational analysis and attempts towards the crystal structure prediction of the anhydrous form. Levofloxacin hemihydrate, CrystEngComm 16 (20) (2014) 4215 ([CrossRef]).
[6] E.M. Gorman, B. Samas, E.J. Munson, Understanding the dehydration of levofloxacin hemihydrate, J. Pharm. Sci. 101 (9) (2012) 3319–3330 ([CrossRef]).
[7] N. Wei, L. Jia, Z. Shang, J. Gong, S. Wu, J. Wang, W. Tang, Polymorphism of levofloxacin: structure, properties and phase transformation, CrystEngComm 21 (41) (2019) 6196–6207 ([CrossRef]).
[8] A.T. Serajuddin, Salt formation to improve drug solubility, Adv. Drug Deliv. Rev. 59 (7) (2007) 603–616 ([CrossRef]).
[9] M. Guo, X. Sun, J. Chen, T. Cai, Pharmaceutical cocrystals: a review of preparations, physicochemical properties and applications, Acta Pharm. Sin. B 11 (8) (2021) 2537–2564 ([CrossRef]).
[10] A. Kolker, J. de Pablo, Thermodynamic modeling of the solubility of salts in mixed Aqueous−Organic solvents, Ind. Eng. Chem. Res. 35 (1) (1996) 228–233 ([Crossref]).
[11] L. Lange, G. Sadowski, Thermodynamic modeling for efficient cocrystal formation, Cryst. Growth Des. 15 (9) (2015) 4406–4416 ([CrossRef]).
[12] F.J. Acebedo-Martínez, A. Domínguez-Martín, C. Alarcón-Payer, A. Sevillano-Páez, C. Verdugo-Escamilla, J.M. González-Pérez, F. Martínez-Checa, D. Choquesillo-Lazarte, Enhanced NSAIDs solubility in drug-drug formulations with ciprofloxacin, Int. J. Mol. Sci. 24 (4) (2023) 3305 ([CrossRef]).
[13] C. Torquetti, P.O. Ferreira, A.C. de Almeida, R.P. Fernandes, F.J. Caires, Thermal study and characterization of new cocrystals of ciprofloxacin with picolinic acid, J. Therm. Anal. 147 (2) (2022) 1299–1306 ([CrossRef]).
[14] N.N. Golovnev, M.S. Molokeev, M.K. Lesnikov, V.V. Atuchin, Two salts and the salt cocrystal of ciprofloxacin with thiobarbituric and barbituric acids: the structure and properties, J. Phys. Org. Chem. 31 (3) (2018) e3773 ([CrossRef]).
[15] T. Shinozaki, M. Ono, K. Higashi, K. Moribe, A novel drug-drug cocrystal of levofloxacin and metacetamol: reduced hygroscopicity and improved photostability of levofloxacin, J. Pharm. Sci. 108 (2019) 2383–2390 ([CrossRef]).
[16] S. Bandari, V.R. Dronam, B.B. Eedara, Development and preliminary characterization of levofloxacin pharmaceutical cocrystals for dissolution rate enhancement, J. Pharm. Investig. 47 (6) (2017) 583–591 ([CrossRef]).
[17] I. Nugrahani, A.N. Laksana, H. Uekusa, H. Oyama, New organic salt from levofloxacin-citric acid: what is the impact on the stability and antibiotic potency? Molecules 27 (7) (2022) 2166 ([CrossRef]).
[18] E.M. Ryan, M.J. Duryee, A. Hollins, S.K. Dover, S. Pirruccello, H. Sayles, K.D. Real, C.D. Hunter, G.M. Thiele, T.R. Mikuls, Antioxidant properties of citric acid interfere with the uricase-based measurement of circulating uric acid, J. Pharm. Biomed. 164 (2019) 460–466 ([CrossRef]).
[19] P. Verma, A. Srivastava, A. Shukia, P. Tandon, M.R. Shimpi, Vibrational spectra, hydrogen bonding interactions and chemical reactivity analysis of nicotinamide-citric acid cocrystal by an experimental and theoretical approach, New J. Chem. 43 (2019) 15956–15967 ([CrossRef]).
[20] M.L.N. Oliveira, R.A. Malagoni, M.R. Franco Jr., Solubility of citric acid in water, ethanol, n-propanol, and in mixtures of ethanol + water, Fluid Phase Equil. 352 (2013) 110–113 ([CrossRef]).
[21] R. Nourmohammadi, N. Afzali, Effect of citric acid and microbial phytase on small intestinal morphology in broiler chicken, Ital. J. Anim. Sci. 12 (2013) e7 ([CrossRef]).
[22] C.C. da Silva, F.F. Guimarães, L. Ribeiro, F.T. Martins, Salt or cocrystal of salt? Probing the nature of multicomponent crystal forms with infrared spectroscopy, Spectrochim. Acta Mol. Biomol. Spectrosc. 167 (2016) 89–95.
[23] J.L. Kee, E.R. Hayes, The United States Pharmacopeia Revision Bulletin 43rd ed., vol. 5, USP 43-NF38); United States Pharmacopeial Convention Inc., Rockville, MD, USA, 2020.
[24] P.A. Wayne, Methods for Dilution Antimicrobial Susceptibility Tests for Bacteria that Grow Aerobically: Approved Standard ninth ed., vol.11, Clinical and Laboratory Standards Institute, Malvern, PA, USA, 2012.
[25] Health Ministry of the Republic of Indonesia, Pharmacopoeia Indonesia V(2), Health Ministry of the Republic Indonesia: Jakarta, Indonesia (2014) 1392–1396.
[26] I. Nugrahani, U. Dwi, I. Slamet, Y.P. Nugraha, H. Uekusa, Zwitterionic cocrystal of diclofenac and L-proline: structure determination, solubility, kinetics of cocrystalization, dan stability study, Eur. J. Pharmaceut. Sci. 117 (2018) 168–176 ([CrossRef]).
[27] A. Czyrski, J. Sznura, The application of box-Behnken-design in the optimization of HPLFCA separation of fluoroquinolones, Sci. Rep. 9 (2019) 19458 ([CrossRef]).
[28] B. Arun, M. Almutairi, N. Komanduri, S. Bandari, F. Zhang, M.A. Repka, Multicomponent crystalline solid forms of aripiprazole produced via hot melt extrusion techniques: an exploratory study, J. Drug Deliv. Sci. Technol. 63 (2021) 102529.

[29] A.C. Almeida, C. Torquetti, P.O. Ferreira, R.P. Fernandes, E.C. dos Santos, A.C. Kogawa, F.J. Caires, Cocrystals of ciprofloxacin with nicotinic and isonicotinic acids: mechanochemical synthesis, characterization, thermal and solubility study, Thermochim. Acta 685 (2020) 178346 ([**Google Scholar**] [CrossRef]).
[30] E. Ayse, E. Eliuz, Antimicrobial activity of citric acid against Escherichia coli, *Staphylococcus aureus* and *Candida albicans* as a sanitizer agent, Eurasian J. For. Sci. 8 (2020) 295–301 ([**Google Scholar**]).
[31] B. Kundukad, G. Udayakumar, E. Grela, D. Kaur, S.S. Rice, S. Kjelleberg, P.S. Doyle, Weak acids as an alternative anti-microbial therapy, Biofilm 2 (2020) 100019 ([**Google Scholar**] [CrossRef] [PubMed]).
[32] W.M. Al-Roussan, N.O. Amin, M.O. Tareq, A.A. Anas, Y.A. Radwan, A.H. Richard, Use of acetic acid and citric acids to inhibit Escherichia coli O157:H7, Salmonella typhimurium and Staphylococcus aureus in tabbouleh salad, Food Microbiol. 73 (2018) 61–66 ([Google Scholar] [CrossRef] [PubMed]).
[33] C. Burel, A. Kala, L. Purevdori-Gage, Impact of pH on citric acid antimicrobial activity against gram-negative bacteria, Lett. Appl. Microbiol. 72 (2021) 332–340 ([**Google Scholar**] [CrossRef] [PubMed]).
[34] R.L. Bunchanan, M.H. Golden, Interaction of citric acid concentration and pH on the kinetics of listeria monocytogenes inactivation, J. Food Protect. 57 (1994) 567–570 ([**Google Scholar**] [CrossRef] [PubMed]).
[35] Memorial Sloan Kattering Cancer Center, Interaction of Sodium citric and citric acid. https://www.mskcc.org/cancer-care/patient-education/medications/adult/sodium-citrate-and-citric-acid?msk_tools_print=pdf, 2022. (Accessed 3 April 2024).